JOURNAL OF SOLID STATE CHEMISTRY 62, 231–240 (1986)

# Topochemical Lithium Insertion into $Fe_2(MoO_4)_3$: Structure and Magnetism of $Li_2Fe_2(MoO_4)_3$

W. M. REIFF* AND J. H. ZHANG

*Department of Chemistry, Northeastern University, Boston, Massachusetts 02115*

AND C. C. TORARDI*

*Central Research and Development Department†, E.I. du Pont de Nemours and Co., Experimental Station, Wilmington, Delaware 19898*

Received June 19, 1985; in revised form September 10, 1985

Powder X-ray diffraction, variable temperature magnetic susceptibility, and zero-field Mössbauer spectroscopy measurements were used to characterize the new phase $Li_2Fe_2(MoO_4)_3$. This material is obtained simply by the mixing of solutions of lithium iodide in acetonitrile with solid $Fe_2(MoO_4)_3$ at ambient temperature. The reaction is entirely reversible using bromine as an oxidant. $Li_2Fe_2(MoO_4)_3$ possesses the high-temperature orthorhombic ferric molybdate structure and Guinier photographs were completely indexed in space group *Pnca* with cell constants $a = 9.3483(5)$, $b = 12.8974(9)$, and $c = 9.4941(6)$ Å versus the monoclinic ($P2_1/a$) $Fe_2(MoO_4)_3$ precursor phase. Chemical analytical data, room-temperature magnetic susceptibility and Mössbauer spectroscopy indicate essentially complete stoichiometric reduction of the latter compound. Magnetic hyperfine splitting of the zero field Mössbauer spectrum below 12.5 K indicates a three-dimensional magnetically ordered state which susceptibility results show to be weakly ferromagnetic owing to probable canting of antiferromagnetically coupled lattices. Above ~40 K, the material obeys a Curie-Weiss law whose parameters are $C = 3.51$ emu/mole, $\mu_{eff} = 5.30\beta$, and $\theta = -19$ K. 

## Introduction

There has been considerable recent interest in intercalation chemistry in general and particularly reactions involving insertion of the smaller Group I metals (Li, Na) into the voids or between the layers of appropriate precursor structures. In addition to the intrinsic interest in this type of basic research in inorganic reaction chemistry, the materials so obtained are potentially important as possible cathode materials for high energy and power density batteries (*1*). For example, the high-temperature electrochemical lithium insertion into $\alpha$-$Fe_2O_3$ has recently been studied in this context (*2*). Lithium insertions under somewhat milder conditions have been done using *n*-butyllithium. We have recently described the synthesis, structure, and low-temperature magnetic properties of the layered system Fe(III)ClMoO$_4$ (*3*). This material undergoes facile topochemical lithium insertion and complete stoichiometric reduction to LiFe(II)ClMoO$_4$ simply on mixing with so-

* To whom correspondence should be addressed.

† Contribution No. 3821.



0022-4596/86 $3.00

lutions of LiI in acetonitrile (*4*). The process is readily reversed with molecular bromine.

Our success with the laycred Fe(III) $ClMoO_4$ stimulated us to attempt lithium insertion into the related three-dimensional network compound $Fe_2(MoO_4)_3$ under mild conditions. This host material has been the subject of several recent X-ray structural studies of which the most definitive is apparently that of Chen (*5*) for which the salient features are now summarized. The compound $Fe_2(MoO_4)_3$ contains exclusively iron(III) and crystallizes in the monoclinic space group $P2_1/a$ with $a = 15.707$, $b = 9.231$, $c = 18.204$ Å, and $\beta = 125.25°$. $Fe(III)O_6$ octahedra and $Mo(VI)O_4$ tetrahedra share only corners in a unit cell whose volume is 2155.5 Å$^3$. The structure of ferric molybdate is related to the garnet structure, $A_3B_2(MO_4)_3$, with the $A$ sites unoccupied. There is also a high-temperature (>499°C) orthorhombic polymorph of $Fe_2(MoO_4)_3$ that will be considered subsequently. The monoclinic form exhibits four crystallographic Fe(III) sites two of which are resolved in the zero-field Mössbauer spectra of the ferrimagnetically ordered phase of the material, i.e., for $T < T_{Néel}$ (13 K) (*6*, *7*). Significantly, the structure is open and "flexible" having large voids between Fe–Mo–O layers. The layers are interconnected by corner shared oxygen atoms. Thus, one can expect rather facile reductive insertion of the smaller alkali metal cations as described in the present paper. Finally, because all coordination polyhedra share only corners, magnetic exchange interactions are expected to be weak and three-dimensional in nature. A preliminary account of this research has been given previously (*8*).

## Experimental

*Synthesis.* Ferric molybdate, $Fe_2(MoO_4)_3$, used as the starting material was synthesized as follows. An aqueous solution of ammonium molybdate was prepared by reacting 25.0 g of $MoO_3$ (0.173 moles) in 100 ml of distilled $H_2O$ with concentrated $NH_4OH$ solution until all the $MoO_3$ was dissolved. To this was added a solution consisting of 46.5 g of $Fe(NO_3)_3 \cdot 9H_2O$ (0.115 moles), 40 g of citric acid (0.208 moles), and 100 ml of distilled $H_2O$. The resulting solution was evaporated to dryness, powdered in a mortar, and carefully heated to 400°C in a muffle furnace. The yellow-green solid was then ground in a mortar and heated at 600°C overnight. This final step was repeated two more times. An X-ray powder diffraction pattern of this preparation showed only the lines of ferric molybdate.

$Li_2Fe_2(MoO_4)_3$ was prepared by reacting 1.0 g of ferric molybdate (1.7 mmole) with a fourfold molar excess of LiI in 50 ml of dry acetonitrile. The reaction was carried out in a Schlenk flask under an argon atmosphere. After stirring at room temperature for 21 days, the orange-brown product was filtered under argon, washed with acetonitrile, dried under vacuum, and transfered to a helium dry box. Chemical analyses established a Fe/Li molar ratio of 1.04, and a Mo/Fe ratio of 1.52. The presence of essentially all $Fe^{2+}$ in $Li_2Fe_2(MoO_4)_3$ was also shown by its Mössbauer spectrum as well as its electronic absorption spectrum (see below).

The insertion of lithium and reduction of $Fe^{3+}$ to $Fe^{2+}$ in ferric molybdate was found to be reversible. Reaction of lithium ferrous molybdate with a threefold excess of $Br_2$ in acetonitrile under inert atmosphere yielded $Fe_2(MoO_4)_3$ after several minutes of stirring at room temperature. This product was characterized by its color and X-ray powder diffraction pattern.

*X-ray powder diffraction.* X-ray powder diffraction patterns were obtained with a Guinier-Hägg-type focusing camera ($r = 40$ mm). The radiation was monochromatic Cu$K\alpha_1$ ($\lambda = 1.5405$ Å) and the internal stan-

dard was Si ($a$ = 5.4305 Å). An Optronics P-1700 Photomation instrument was used to collect absorbance data from the films. Peak positions and relative intensities were determined with local computer programs. $Li_2Fe_2(MoO_4)_3$ was indexed as orthorhombic by the Visser program (*9*) using the first 20 lines of the pattern. The lattice parameters were subsequently refined with local computer programs. An excellent refinement was obtained using all 78 observed lines. $Li_2Fe_2(MoO_4)_3$ was found to be orthorhombic with $a$ = 9.3483(5), $b$ = 12.8974(9), and $c$ = 9.4941(6) Å. The indexed X-ray powder diffraction pattern recorded under vacuum at ambient temperature is given in Table I. The figures of merit (*10, 11*) for this indexing are: $M_{20}$ = 99 and $F_{20}$ = 93(0.008,27). Calculated intensities for $Li_2Fe_2(MoO_4)_3$ were approximated by using the positional parameters of orthorhombic scandium tungstate (*12*), $Sc_2(WO_4)_3$, for Fe, Mo, and O, and the above lattice parameters with space group *Pnca*. Lithium was not included. This is discussed in more detail below.

*Magnetic susceptibility and Mössbauer spectroscopy.* Magnetic susceptibility and Mössbauer spectra measurements were determined as described previously (*13*). All analytical measurements were done for samples sealed in an atmosphere of argon or helium.

TABLE I

X-RAY POWDER DIFFRACTION DATA FOR $Li_2Fe_2(MoO_4)_3$

| 2θ | I(obs) | I(calc)[a] | hkl | d(obs) | d(calc) |
|---|---|---|---|---|---|
| 13.745 | 11 | 12 | 0 2 0 | 6.437 | 6.449 |
| 14.965 | 17 | 32 | 1 1 1 | 5.915 | 5.918 |
| 19.148 | 15 | 10 | 1 2 1 | 4.631 | 4.633 |
| 20.189 | 36 | 30 | 2 1 0 | 4.395 | 4.394 |
| 20.973 | 69 | 53 | 1 0 2 | 4.232 | 4.233 |
| 22.084 | 75 | 44 | 1 1 2 | 4.022 | 4.022 |
| 22.286 | 69 | 40 | 2 1 1 | 3.986 | 3.988 |
| 22.691 | 100 | 100 | 0 3 1 | 3.915 | 3.916 |
| 23.256 | 22 | 8 | 0 2 2 | 3.822 | 3.823 |
| 23.476 | 13 | 13 | 2 2 0 | 3.786 | 3.785 |
| 24.623 | 19 | 26 | 1 3 1 | 3.612 | 3.612 |
| 25.306 | 74 | 56 | 2 2 1 | 3.516 | 3.516 |
| 26.737 | 34 | 40 | 2 0 2 | 3.331 | 3.331 |
| 27.633 | 37 | 7 | 2 1 2 | 3.225 | 3.225 |
| | | 14 | 0 4 0 | | 3.224 |
| 29.023 | 23 | 17 | 0 1 3 | 3.074 | 3.074 |
| 29.597 | 17 | 6 | 1 3 2 | 3.016 | 3.016 |
| 29.712 | 12 | 10 | 2 3 1 | 3.004 | 3.002 |
| 30.172 | 22 | 11 | 2 2 2 | 2.959 | 2.959 |
| 30.770 | 11 | 4 | 1 4 1 | 2.903 | 2.902 |
| 30.959 | 42 | 16 | 3 1 1 | 2.886 | 2.886 |
| 32.922 | 63 | 28 | 1 2 3 | 2.718 | 2.718 |
| 33.253 | 13 | 11 | 3 2 1 | 2.692 | 2.691 |
| 33.563 | 9 | 4 | 0 4 2 | 2.668 | 2.667 |
| 33.749 | 23 | 11 | 2 4 0 | 2.654 | 2.654 |
| 34.367 | 3 | 7 | 3 0 2 | 2.607 | 2.605 |
| 34.921 | 7 | 4 | 2 1 3 | 2.567 | 2.568 |
| | | 3 | 1 4 2 | | 2.565 |
| 35.079 | 9 | 3 | 2 4 1 | 2.556 | 2.556 |
| | | 3 | 3 1 2 | | 2.553 |
| 36.509 | 18 | 16 | 1 3 3 | 2.459 | 2.459 |
| 36.816 | 3 | 3 | 3 3 1 | 2.439 | 2.438 |
| 39.125 | 7 | 1 | 1 0 4 | 2.300 | 2.301 |
| | | 1 | 4 1 0 | | 2.300 |
| 39.881 | 17 | 5 | 2 5 0 | 2.259 | 2.258 |
| 40.312 | 25 | 15 | 4 1 1 | 2.235 | 2.235 |

Plus 46 lines to $d$ = 1.276

[a] See text.

## Results

### *Synthesis and Structure*

Preparation of $Li_2Fe_2(MoO_4)_3$ by chemical and electrochemical methods has been described recently (*14*). Both involved the insertion of lithium ions into the ferric molybdate structure with concurrent reduction of ferric to ferrous ions. The reported chemical method involved rapid reaction of $Fe_2(MoO_4)_3$ with *n*-butyllithium in hexane. We report that $Li_2Fe_2(MoO_4)_3$ can also be prepared from ferric molybdate in a non-aqueous solution of lithium iodide via the reaction

$$\underset{\text{(solid)}}{Fe_2(MoO_4)_3} + \underset{\text{(solution)}}{2\ LiI} \xrightarrow{CH_3CN} \underset{\text{(solid)}}{Li_2Fe_2(MoO_4)_3} + \underset{\text{(solution)}}{I_2}$$

Compared to the *n*-butyllithium reaction,

the lithium iodide reaction is milder and requires a longer time to attain full iron reduction at ambient temperature. This is understood by comparing the EMF vs $Li/Li^+$ for the two reagents: ~1 V for *n*-butyllithium and 2.8 V for LiI. Analogous results have recently been obtained on the layered compound Fe(III)$ClMoO_4$ (*3*, *4*) where reaction with LiI in acetonitrile gives LiFe(II) $ClMoO_4$. Under vacuum at 200°C, $Li_2Fe_2(MoO_4)_3$ transforms to another more stable orthorhombic modification (*15*, *16*).

The present work shows that $Li_2Fe_2(MoO_4)_3$ possesses the high-temperature orthorhombic $Fe_2(MoO_4)_3$ structure. In contrast, the low-temperature monoclinic form of ferric molybdate was reported for the *n*-butyllithium and electrochemical preparations (*14*). Due to the lack of significant figures and standard deviations for the reported monoclinic cell of $Li_2Fe_2(MoO_4)_3$, and the closely related X-ray powder diffraction pattern of monoclinic $Fe_2(MoO_4)_3$, it is assumed that the latter preparations are also orthorhombic. This structure has been shown to exist for several $A_2^{3+}(MO_4)_3$ compounds ($A$ = Al, Cr, Fe, In, Sc, and Lu with $M$ = Mo; A = Al, In, Sc, Lu, and Yb with $M$ = W) (*17*). Consistent with the insertion of $Li^+$ and reduction of iron to the larger $Fe^{2+}$ ion, the doubled unit cell volume of $Li_2Fe_2(MoO_4)_3$ is 6.2% greater than that of the ferric phase. Unit cell parameters of the orthorhombic $Li_2Fe_2(MoO_4)_3$ and monoclinic $Fe_2(MoO_4)_3$ structures are related as follows:

$$\begin{pmatrix} a \\ b \\ c \end{pmatrix}_{\text{ortho}} = \begin{pmatrix} 0 & 0 & -\frac{1}{2} \\ -1 & 0 & -\frac{1}{2} \\ 0 & 1 & 0 \end{pmatrix} \begin{pmatrix} a \\ b \\ c \end{pmatrix}_{\text{mono}}.$$

Using the positional coordinates and space group (*Pnca*) of orthorhombic $Sc_2(WO_4)_3$ (*12*) for Fe, Mo, and O, and the observed unit cell parameters for $Li_2Fe_2(MoO_4)_3$, a calculated X-ray powder diffraction pattern was obtained. Table I compares the observed Guinier X-ray film intensities with the calculated values. The qualitatively good fit between these intensities indicates the model is essentially correct. Even if the lithium atom positions were known, the calculated intensities would not change very much due to the low X-ray scattering power of lithium. Reasonable interatomic distances and angles were also calculated from the unrefined atomic positions.

The structure of $Li_2Fe_2(MoO_4)_3$ contains layers of corner-shared $FeO_6$ octahedra and $MoO_4$ tetrahedra oriented in the *ac* plane (Fig. 1). Each oxygen atom is bonded to one Mo and one Fe atom. Layers are interconnected by oxygen atoms shared between $FeO_6$ octahedra of one layer and $MoO_4$ tetrahedra of an adjacent layer. Only one crystallographic iron atom is present in this structure. Although the point group symmetry for the $FeO_6$ groups is $C_1$, the octahedra are close to being regular. There are two crystallographic molybdenum atoms: one has each of its four O atoms bonding to Fe atoms within a layer, the other has one O atom connecting to an Fe atom in a neighboring layer. The open framework allows lithium ions to easily move topotactically in and out of the structure. Lithium ions may occupy sites between or within the layers. The ions could be disordered

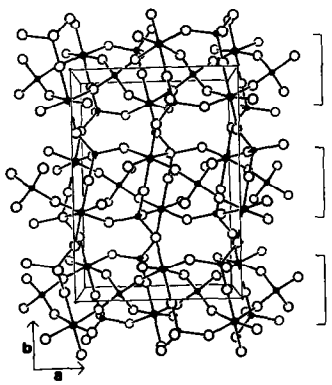


FIG. 1. A view along the *c* axis of $Li_2Fe_2(MoO_4)_3$ showing the Fe–Mo–O layers interconnected by shared O atoms.

over distorted "8-coordinate" $A$ sites of the $A_3B_2(MO_4)_3$ garnet structure or ordered over two-thirds of these sites. These sites may be distorted in a manner which yields lower coordination positions that would be more favorable for the small lithium ions (i.e., 6 or 4 coordination).

*Near Infrared-Visible Spectrum*

Mull diffuse reflectance spectra of $Fe_2(MoO_4)_3$ and $Li_2Fe_2(MoO_4)_3$ are shown in Fig. 2. The $Fe_2(MoO_4)_3$ precursor material corresponds to a $^6A$ ground term in an $Fe(III)O_6$ chromophore. For this moiety, the lowest energy intrametal ($d$–$d$) transition is usually $\gtrsim$10,000 $cm^{-1}$ and is the spin and Laporte forbidden $^6A \rightarrow {}^4T$ band at ~11,360 $cm^{-1}$ in the figure. For $Fe^{2+}$ in $Li_2Fe_2(MoO_4)_3$, the ground term is a nominal $^5T(O_h)$ and, in the absence of a significant low-symmetry ligand field component band splitting effect, one single electron spin allowed Laporte forbidden $d$–$d$ transition ($^5T \rightarrow {}^5E$) is expected. Figure 2 clearly shows this. The centroid of the band system which is definitely more intense than that for the precursor is at ~7500 $cm^{-1}$. The two components are centered at ~6670 and ~8330 $cm^{-1}$ and thus the excited state ($^5E$) splitting is estimated to be ~1660 $cm^{-1}$. In light of the fact that the $Fe(II)O_6$ octahedra are fairly regular, it seems likely that the band splitting has its origin in a Jahn-Teller effect (*18*). The centroid can be taken as a rough estimate of the 10 Dq crystal field splitting factor for the $Fe(II)O_6$ chromophore. This is to be compared to 10 Dq as determined by optical spectra for an aqueous solution of a system such as $Fe(H_2O)_6^{2+}$ for which the $^5T \rightarrow {}^5E$ transition is similarly split (~2000 $cm^{-1}$). Its centroid occurs at ~10,000 $cm^{-1}$ (*18*) and indicates a somewhat larger 10 Dq for the $Fe(H_2O)_6^{2+}$ ion than the present condensed $Fe(II)O_6$ chromophore. This is not unreasonable in view of the fact that all of the oxygen atoms are terminal monodentate ligands in the former and bridging ligands in the latter, hence leading to a weaker ligand field in the condensed phase.

*Zero-Field Mössbauer Spectroscopy*

Some zero-field Mössbauer spectra are presented in Figs. 3 and 4 for a number of temperatures above and below an apparent three-dimensional ordering temperature ($T_{critical}$) where $12.0 < T_c < 12.5$ K. Sample data are given in Table II. Spectra above and below $T_c$ are best fit for a single quadrupole doublet (two Lorentzians) and a single Zeeman hyperfine pattern (six Lorentzians), respectively. Some spectral asymmetry (slightly more intense transition at

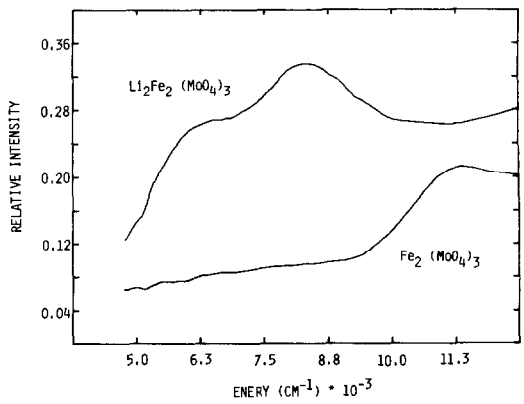


FIG. 2. The electronic absorption spectra of $Li_2Fe_2(MoO_4)_3$ and $Fe_2(MoO_4)_3$.

TABLE II

SOME ZERO-FIELD MÖSSBAUER SPECTROSCOPY PARAMETERS[a] FOR $Li_2Fe_2(MoO_4)_3$, $T > T_{Néel}$

| $T$(K) | $\delta$ | $\Delta E$ |
|---|---|---|
| 293 | 1.026 | 0.825 |
| 77.4 | 1.164 | 1.559 |
| 20.0 | 1.172 | 1.683 |
| 13.0 | 1.171 | 1.709 |
| 12.5 | 1.171 | 1.722 |

[a] mm/sec relative to natural iron foil.

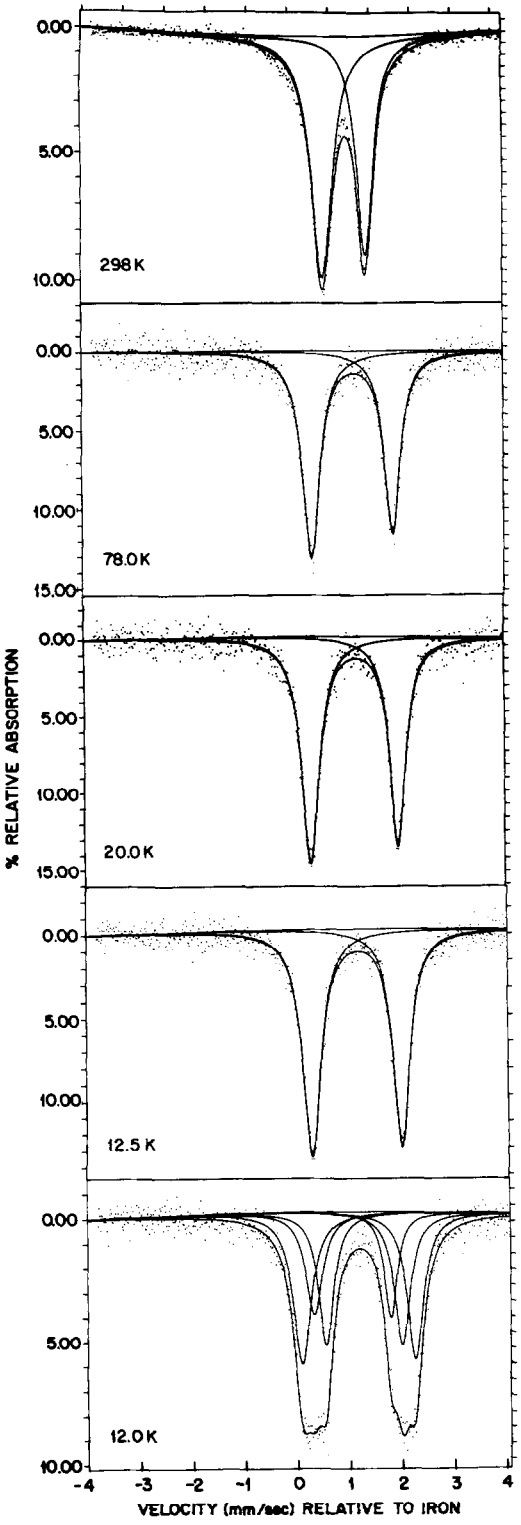


FIG. 3. Mössbauer spectra of $Li_2Fe_2(MoO_4)_3$ above $T_{Néel}$ (12.5 K).

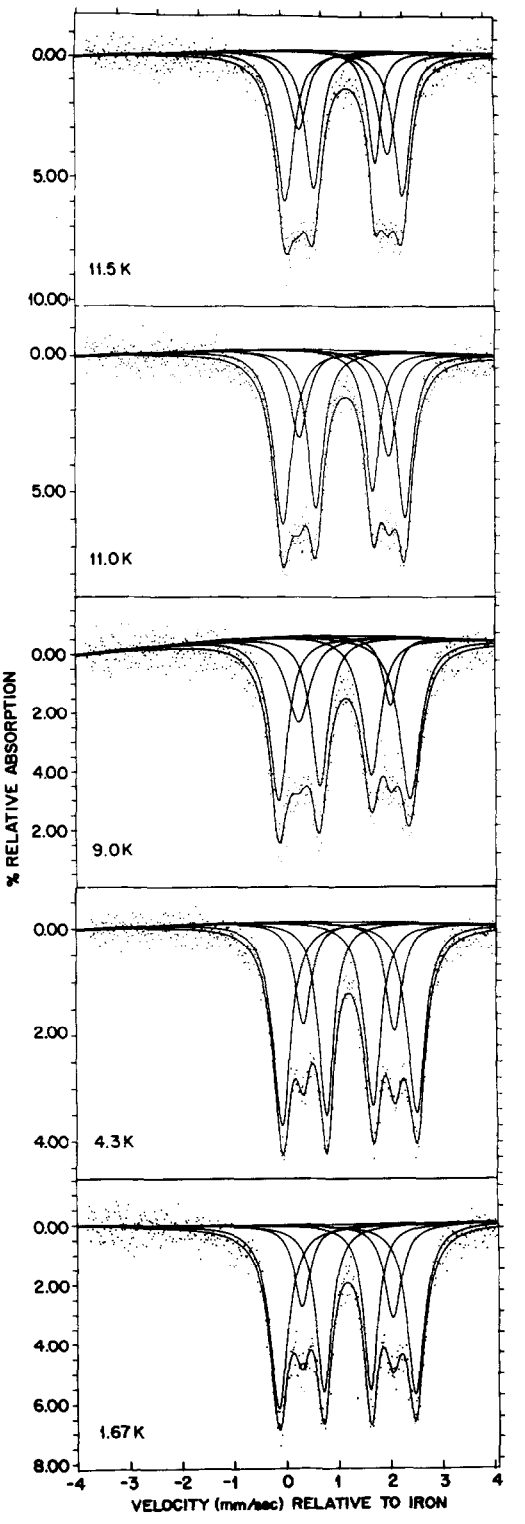


FIG. 4. Mössbauer spectra of $Li_2Fe_2(MoO_4)_3$ below $T_{Néel}$ (12.5 K).

lower velocity) is evident at all temperatures $T > T_c$ suggesting sample texture (nonrandomness) and/or trace ferric impurity. The latter could result from incomplete reaction of the $Fe_2(MoO_4)_3$ with LiI and/or oxidation of the $Li_2Fe_2(MoO_4)_3$ product. The possible ferric impurity is estimated to be at most ~1% based on the area difference between the high- and low-velocity transitions and assuming that the spectrum of the ferrous contribution is symmetric. To avoid atmospheric exposure and decomposition, no attempt was made to overcome texture by usual sample pulverization–randomization techniques. Mössbauer lines are slightly broadened with widths of the order of 0.35 mm due to a combination of ferric impurity and environmental broadening (local vibrations) for our particular cryogenic sample mount. There was no evidence from goodness of fit values or residual plots (which are generally quite random) to indicate more than one iron environment.

The isomer shift is typical of high-spin iron(II) in an $FeO_6$ ligand chromophore. The ambient and limiting low-temperature values of the quadrupole splitting are small for high-spin iron(II) and suggest a relatively undistorted symmetric coordination environment. This apparently leads to a large unquenched orbital contribution ($H_L$) to the internal hyperfine field ($H_{int}$), vide infra. The room-temperature quadrupole splitting of the precursor $Fe_2(MoO_4)_3$ is only 0.18 mm/sec. In view of the fact that $^6A$ ground state high-spin ferric is involved, the foregoing splitting has its origin in a small "lattice" contribution to the electric field gradient. In contrast, the highly temperature dependent quadrupole splitting of $Li_2Fe_2(MoO_4)_3$ is typical of a dominant valence contribution to the electric field gradient as expected for iron(II) in an "undistorted" environment. In view of the temperature dependence to $\Delta E$, the $t_{2g}$ manifold splitting is estimated to be $<\sim 500$ $cm^{-1}$ while the limiting value of $\Delta E$ (~1.7 mm/sec) suggests a nominal $^5E$ ground term, i.e., an orbital doublet ground state.

The Mössbauer spectrum undergoes a sharp transition to a magnetic hyperfine split pattern between 12.5 and 12 K corresponding to a cooperative three-dimensional magnetic ordering process as opposed to any kind of gradual single-ion slow paramagnetic relaxation. This view and a critical temperature between 12 and 12.5 K are confirmed by susceptibility results to be considered subsequently. The limiting shape of the hyperfine pattern deserves additional comment. The typical observation is a symmetric ~3 : 2 : 1 : 1 : 2 : 3 pattern with perhaps a quadrupolar shift of the center of the inner four $\gamma$-ray transitions relative to the center of the outer two depending on the angle between $V_{zz}$ and $H_{int}$. This is expected for the case of a Zeeman splitting perturbation that is large compared to the quadrupole interaction, i.e., $H_{int} \gg V_{zz}$ and is exactly what is observed for the precursor $Fe_2(MoO_4)_3$ in its ferrimagnetically ordered state, i.e., $T < 12 \pm \sim 1$ K and for which the limiting value of $H_{int}$ is ~530 kOe. The limiting low-temperature Mössbauer spectrum of $Li_2Fe_2(MoO_4)_3$ should be viewed in terms of the following general considerations. First of all, the internal hyperfine field ($H_{int}$) is composed primarily of three contributions: (1) $H_C$, Fermi contact (~110 kOe/spin); (2) $H_D$, the dipolar contribution; and (3) $H_L$, an orbital contribution, i.e., $H_{int} = H_C + H_D + H_L$. For sextet $Fe^{3+}$, (1) is clearly dominant. For quintet $Fe^{2+}$, $H_C$ is expected to be smaller owing to one less spin and greater covalency reduction effects for $Fe^{2+}$. In addition, $H_L$ can now be large especially for cases of small quadrupole splitting, and is of *opposite sign* to $H_C$. The rather small limiting value of $H_{int}$ (~110 kOe) for $Li_2Fe_2(MoO_4)_3$ is entirely consistent with a combination of these effects. The shape of the observed Mössbauer spectrum is more nearly like that predicted for

the perturbation scheme $V_{zz} \gtrsim H_{int}$ with $\eta$, the asymmetry parameter, ~1.

In passing, we conclude this section by pointing out that (save for isomer shifts) the Mössbauer parameters and low-temperature spectral behavior of $Li_2Fe_2(MoO_4)_3$ are quite unlike those observed (*19*) for the various polymorphs of $Fe(II)MoO_4$ which also contain six coordinate Fe(II). This is reassuring in the context of further distinguishing the new phase reported herein from other possible products. Finally, the low-temperature magnetic behavior of $Li_2Fe_2(MoO_4)_3$ to be discussed now is similarly quite different from that published (*19*) for the preceding $Fe(II)MoO_4$ polymorphs.

*Magnetic Susceptibility*

The magnetic susceptibility results for $Li_2Fe_2(MoO_4)_3$ are presented in Figs. 5 and 6 for the temperature ranges 300 to 26 K and 1.6 to 100 K, respectively. Magnetic moment values ($H_0$ = 5.1 kG) steadily decrease from 5.10$\beta$ at 291 K to 3.87$\beta$ at 25.8 K. Below the latter temperature, the moment becomes field dependent as shown in Fig. 6. The Curie-Weiss parameters obtained from least-squares fits of $\chi_m^{-1} = T - \theta/C$ for the high-temperature data set are $\theta$ = −19.38 K, $C$ = 3.508 em$\mu$/mole and $\mu$(effective) = 5.29$\beta$. From the moment variation shown in the high-temperature data set and the sign of $\theta$, it is clear that the *dominant magnetic exchange interaction is antiferromagnetic* in nature. The moment ($\mu$) has decreased more than a full Bohr magneton unit below the spin-only value ($\mu_{s.o.} = (4s(s+1))^{1/2}$, i.e., $g$ = 2) expected (~4.9$\beta$) for spin quintet ferrous. In the low-temperature data set there is a sharp rise in $\mu$ and pronounced field dependent behavior ($\chi$ inverse to $H_0$) characteristic of the generation of a spontaneously magnetized *three dimensional ferromagnetic ground state.* The onset of the field dependence and rapid

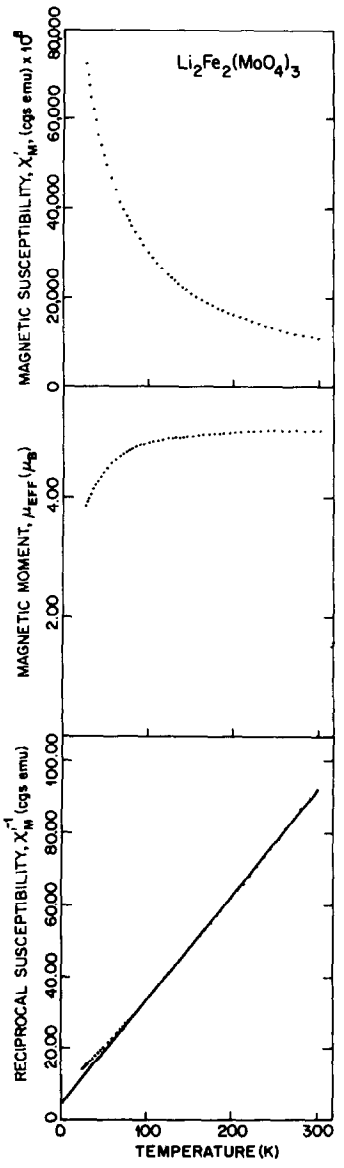


FIG. 5. Magnetic susceptibility data for $Li_2Fe_2(MoO_4)_3$ in the range 26 to 300 K, $H_0$ = 5.1 kG.

rise in $\mu$ occur at ~12 K coincident with the sudden magnetic hyperfine splitting of the zero field Mössbauer spectrum. Based on the inflection in $\chi'_m$ vs $T$ and the onset of Zeeman splitting of zero-field Mössbauer spectra, we estimate $T_{critical}$ (act-

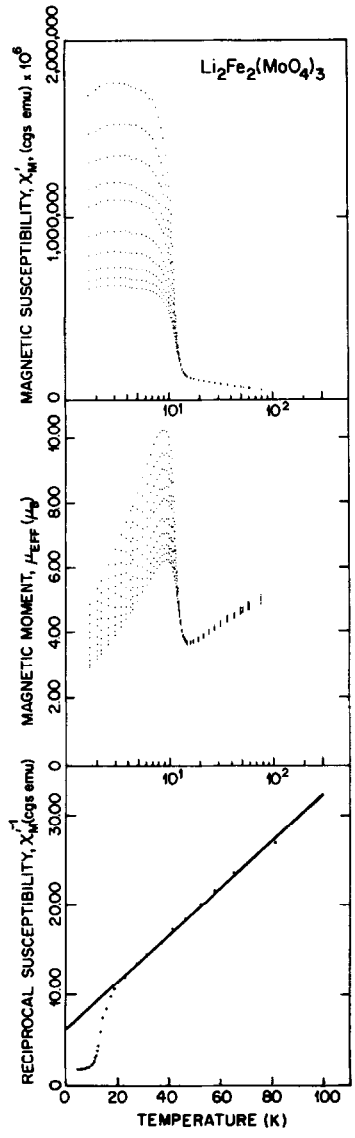


FIG. 6. Magnetic susceptibility data for $Li_2Fe_2(MoO_4)_3$ in the range 1.6 to 100 K, $H_0$ = 1.6 kG (top), 5.1 kG (bottom).

ually $T_{Néel}$ in view of $\theta$ negative) to be 12 ± 0.5 K.

## Discussion

The details of the magnetic structure and $Li^+$ cation location must await single crystal X-ray structure and susceptibility study and/or neutron diffraction[1] at various temperatures. However, one can make the following general comments concerning some aspects of these problems with some confidence based on the presently available powder data. First of all, since the Néel temperatures of the new lithiated phase and the $Fe_2(MoO_4)_3$ precursor are essentially identical, and the paramagnetic curie temperature of similar magnitude (for $Fe_2(MoO_4)_3$ $\theta = -55.6$ K), one concludes that the basic structure and magnetic exchange network of $Fe_2(MoO_4)_3$ are little altered on lithium insertion save of course for metal ion reduction. From the observation that there is only *one type* of iron apparent in the Mössbauer spectra at all temperatures and that *all* the iron atoms are equivalent in the orthorhombic space group derived from indexing the room-temperature Guinier data, it is clear that $Li_2Fe_2(MoO_4)_3$ cannot be properly classified as a ferrimagnet. This contrasts with the monoclinic form of the precursor $Fe_2(MoO_4)_3$ and likewise $Fe_2(SO_4)_3$ ($T_{Néel} \sim 29$ K) which have been shown to be *L*-type ferrimagnets with truely inequivalent metal atoms. Yet there is clearly a high moment spontaneously magnetized state for $Li_2Fe_2(MoO_4)_3$ for $T < \sim 12$ K, i.e., a weak ferromagnet. On the basis of the present data, we conclude that this state probably arises from some type of canting of equivalent, antiferromagnetically coupled sublattices leading to a nonzero resultant moment in the three-dimensionally ordered state.

[1] *Note added in proof.* We have now refined the structure of $Li_2Fe_2(MoO_4)_3$ from powder neutron diffraction data (*20*). Interlayer lithium-ion sites are ordered and fully occupied. Lithium is tetrahedrally coordinated to oxygen by bridging the edges of two $FeO_6$ octahedra. Determination of the neurton magnetic structure at 4.2 K as well as high field Mössbauer and magnetization studies is in progress (*21*).

## Acknowledgments

The authors thank C. M. Foris for obtaining the Guinier data, and Mr. M. W. Sweeten for technical assistance. W. M. Reiff is pleased to acknowledge the support of the National Science Foundation, Division of Materials Research, Solid State Chemistry Program, Grant DMR 8313710.

## References

1. D. W. Murphy and P. A. Christian, *Science* **205,** 651 (1979).
2. M. M. Thackeray, W. I. F. David, and J. B. Goodenough, *J. Solid State Chem.* **55,** 280 (1984).
3. C. C. Torardi, J. C. Calabrese, K. Lázár, and W. M. Reiff, *J. Solid State Chem.* **51,** 376 (1984).
4. C. C. Torardi, K. Lázár, W. M. Reiff, and E. Prince, submitted to *J. Phys. Chem. Solids.*
5. H.-Y. Chen, *Mat. Res. Bull.* **14,** 1583 (1979).
6. Z. Jirak, R. Salmon, L. Fournes, F. Menil, and P. Hagenmuller, *Inorg. Chem.* **21,** 4218 (1982).
7. P. D. Battle, A. K. Cheetham, G. J. Long, and G. Longworth, *Inorg. Chem.* **21,** 4223 (1982).
8. C. C. Torardi, W. M. Reiff, and J.-H. Zhang, Inorganic Paper No. 158, National A.C.S. Meeting, Philadelphia, Pa., August 1984.
9. J. W. Visser, *J. Appl. Crystallogr.* **2,** 89 (1969).
10. P. M. de Wolff, *J. Appl. Crystallogr.* **1,** 108 (1968).
11. G. S. Smith and R. L. Snyder, *J. Appl. Crystallogr.* **12,** 60 (1979).
12. S. C. Abrahams and J. L. Bernstein, *J. Chem. Phys.* **45,** 2745 (1966).
13. C. Cheng and W. M. Reiff, *Inorg. Chem.* **16,** 2097 (1977).
14. A. Nadiri, C. Delmas, R. Salmon, and P. Hagenmuller, *Rev. Chim. Miner.* **21,** 537 (1984).
15. P. V. Klevtsov, *Sov. Phys. Crystallogr.* **15,** 682 (1971).
16. R. F. Klevtsova and S. A. Magarill, *Sov. Phys. Crystallogr.* **15,** 611 (1971).
17. A. W. Sleight and L. H. Brixner, *J. Solid State Chem.* **7,** 172 (1973).
18. B. N. Figgis, "Introduction to Ligand Fields," p. 225, Wiley-Interscience, New York, 1966.
19. A. W. Sleight, B. L. Chamberland, and J. F. Weiher, *Inorg. Chem.* **7,** 1093 (1968).
20. C. C. Torardi and E. Prince, *Mat. Res. Bull.*, in press.
21. C. C. Torardi, W. M. Reiff, J. H. Zhang, and E. Prince, to be published.